SUPPLEMENTARY MATERIALS FOR "AN UNSUPERVISED DEEP APPROACH FOR REAL-WORLD IMAGE DENOISING"

Anonymous authors
Paper under double-blind review

1 VISUAL RESULTS ON REAL WORLD NOISE

We show visual results on nature real world noise dataset in 1.1 and real fluorescence microscopy dataset in 1.2. Moreover, ten real noisy images are captured by consumer cameras with ISO=3200 or 320. Similar to the CC dataset, we crop a 512×512 region in each image to evaluate the performance NN+BM3D, see 1.3.

1.1 VISUAL EXAMPLE OF CC, POLYU

We show visual results of ten noisy images from CC (Nam et al., 2016) and PolyU (Xu et al., 2018a) datasets. BM3D (Dabov et al., 2007), DnCNN (Zhang et al., 2017), NC (Lebrun et al., 2015), MCWNNM (Xu et al., 2017) and TWSC (Xu et al., 2018b) are evaluated for comparison. See CC's results in page 2, 3 and PolyU's results in page 4, 5.

1.2 VISUAL EXAMPLE OF FMDD

Two images from FMDD Zhang et al. (2019) datasets are evaluated for visual comparisons. We compared our approach with VST method (Makitalo & Foi, 2012), See page 6.

1.3 VISUAL EXAMPLES OF REAL IMAGE

Ten real noisy images are evaluated for visual comparisons. The results of three traditional methods (BM3D (Dabov et al., 2007), MCWNNM (Xu et al., 2017) and NC (Lebrun et al., 2015)) and three deep learning methods (VDN (Yue et al., 2019), DnCNN (Zhang et al., 2017) and FFDNet (Zhang et al., 2018)) are shown here. See Figure 4 in page 7, 8, 9.

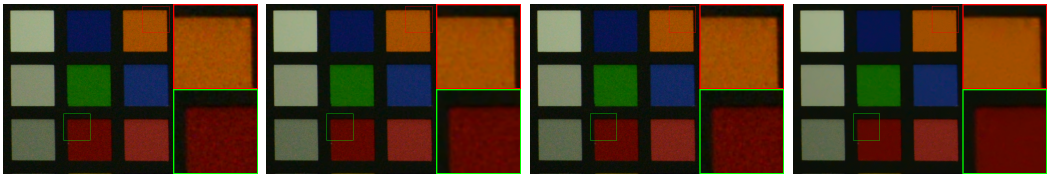

(a) Noisy 34.93/0.8406 (b) BM3D 37.18/0.9113 (c) DnCNN 35.73/0.8588 (d) NC 39.29/0.9536

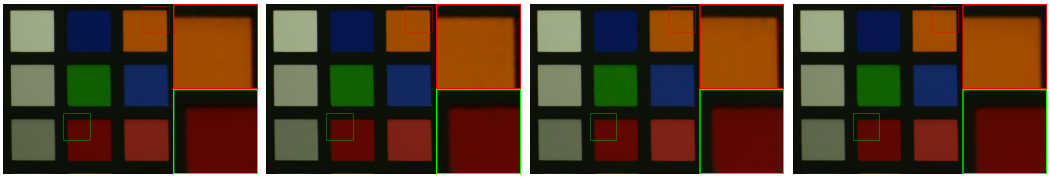

(e) Ground Truth (f) MCWNNM 41.15/0.9774 (g) TWSC 41.05/0.9831 (h) NN+BM3D **42.63/0.9858**

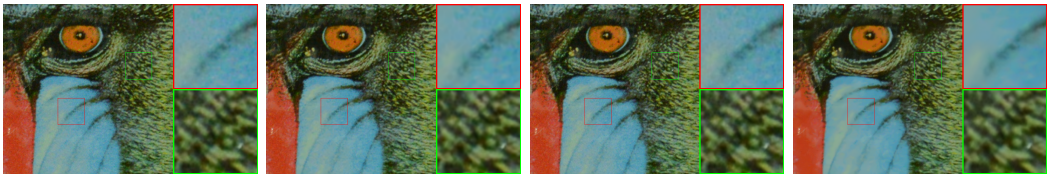

(a) Noisy 33.28/0.8996 (b) BM3D 34.60/0.9324 (c) DnCNN 33.95/0.9112 (d) NC 35.57/0.9479

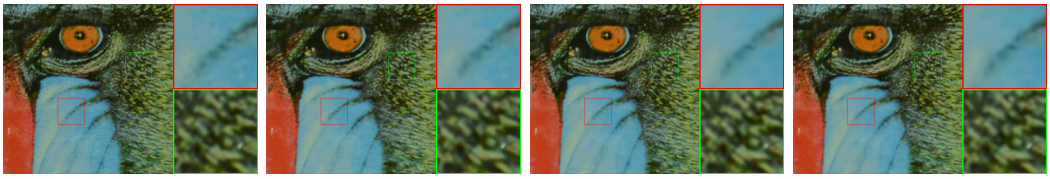

(e) Ground Truth (f) MCWNNM 34.98/0.9469 (g) TWSC 35.34/0.9547 (h) NN+BM3D **35.80/0.9555**

(a) Noisy 33.88/0.8943 (b) BM3D 35.38/0.9360 (c) DnCNN 34.21/0.9013 (d) NC 35.60/0.9399

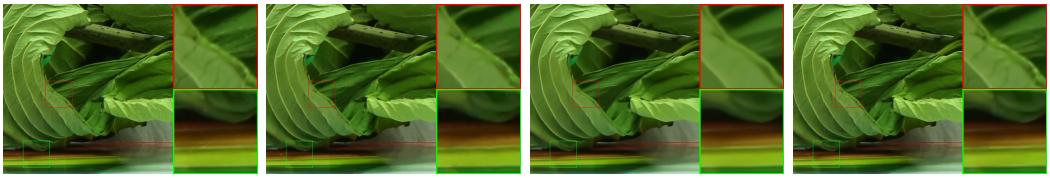

(e) Ground Truth (f) MCWNNM 35.37/0.9328 (g) TWSC 35.90/0.9328 (h) NN+BM3D **37.32/0.9590**

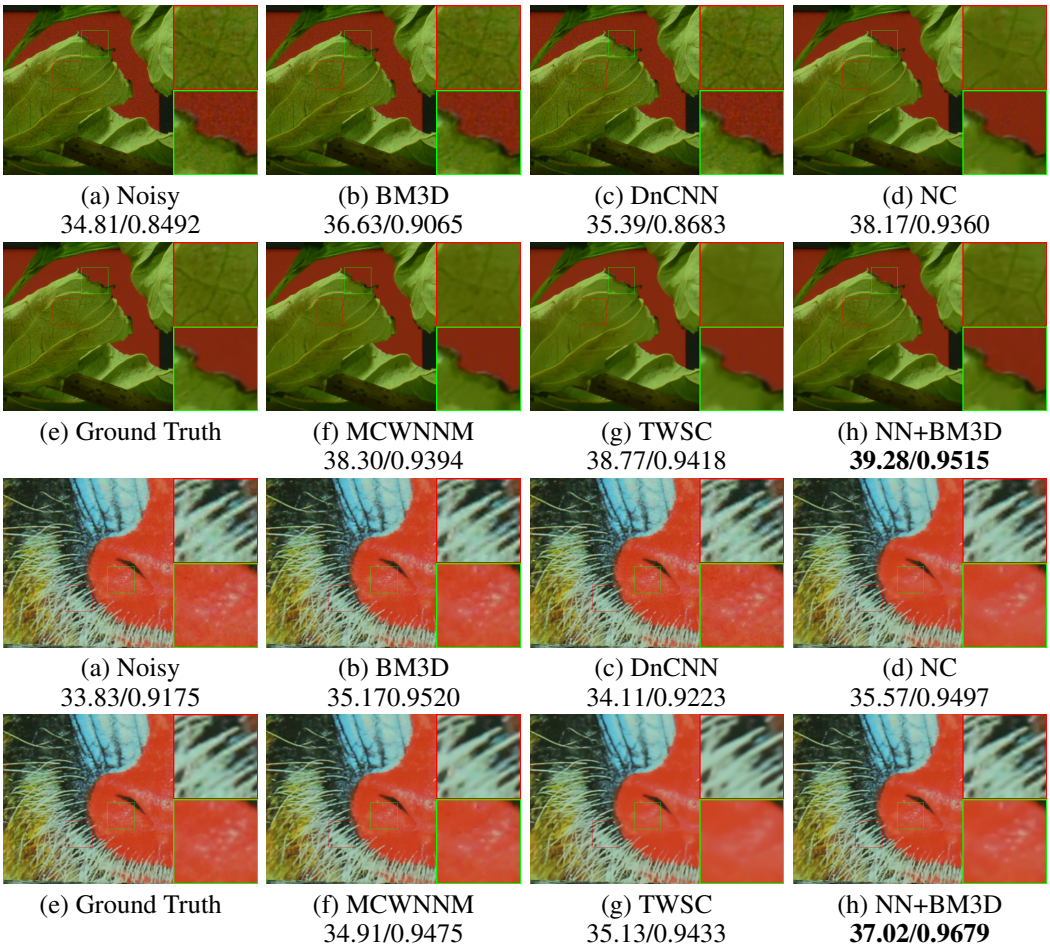

Figure 1: Visual results and PNSR/SSIM of five noisy images from CC.

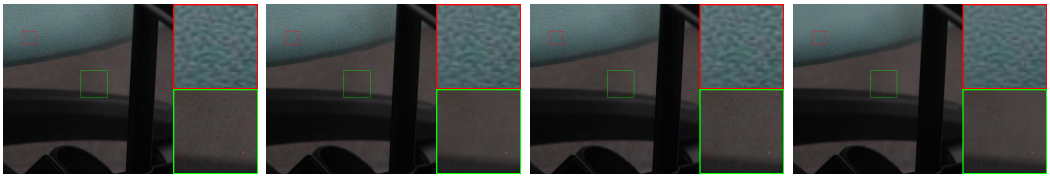

(a) Noisy 36.79/0.9165 (b) BM3D 37.68/0.9442 (c) DnCNN 36.83/0.9199 (d) NC 37.70/0.9373

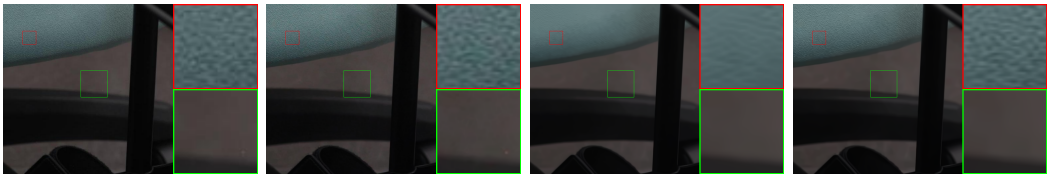

(e) Ground Truth (f) MCWNNM 38.42/0.9534 (g) TWSC 37.82/0.9269 (h) NN+BM3D **38.95/0.9590**

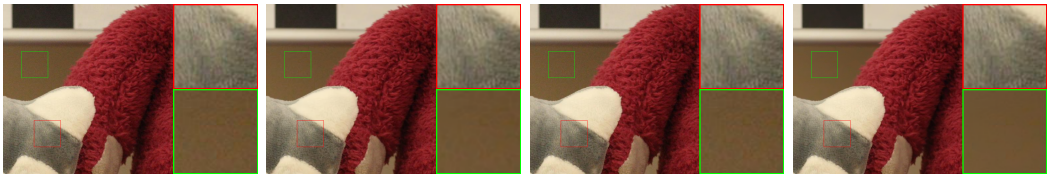

(a) Noisy 36.42/0.9198 (b) BM3D 37.39/0.9422 (c) DnCNN 36.58/0.9227 (d) NC 37.34/0.9405

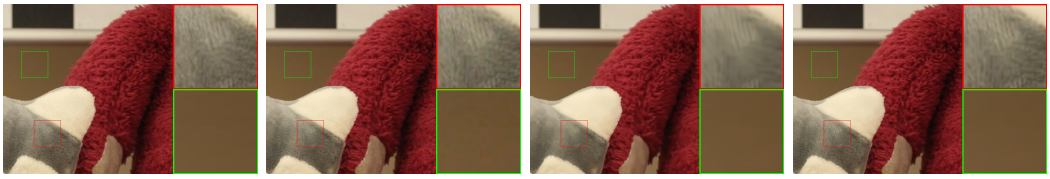

(e) Ground Truth (f) MCWNNM 37.94/0.9501 (g) TWSC 37.47/0.9340 (h) NN+BM3D **38.31/0.9538**

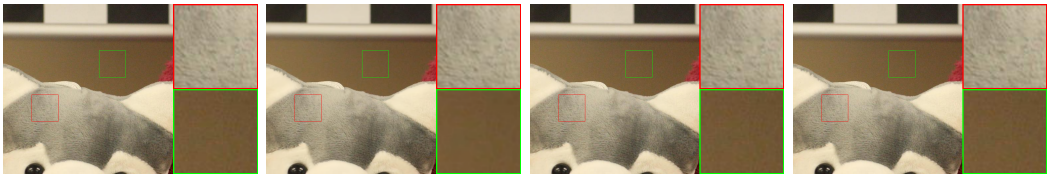

(a) Noisy 36.88/0.9240 (b) BM3D 37.87/0.9474 (c) DnCNN 37.06/0.9279 (d) NC 36.88/0.9240

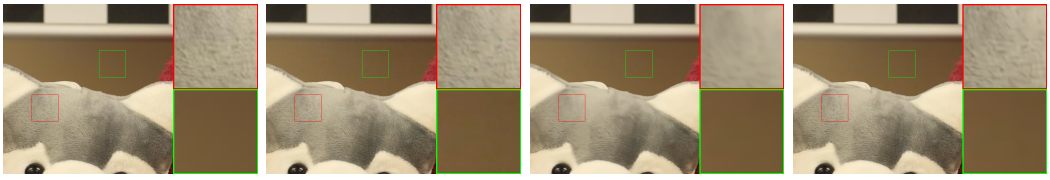

(e) Ground Truth (f) MCWNNM 38.43/0.9552 (g) TWSC 37.37/0.9273 (h) NN+BM3D **38.80/0.9582**

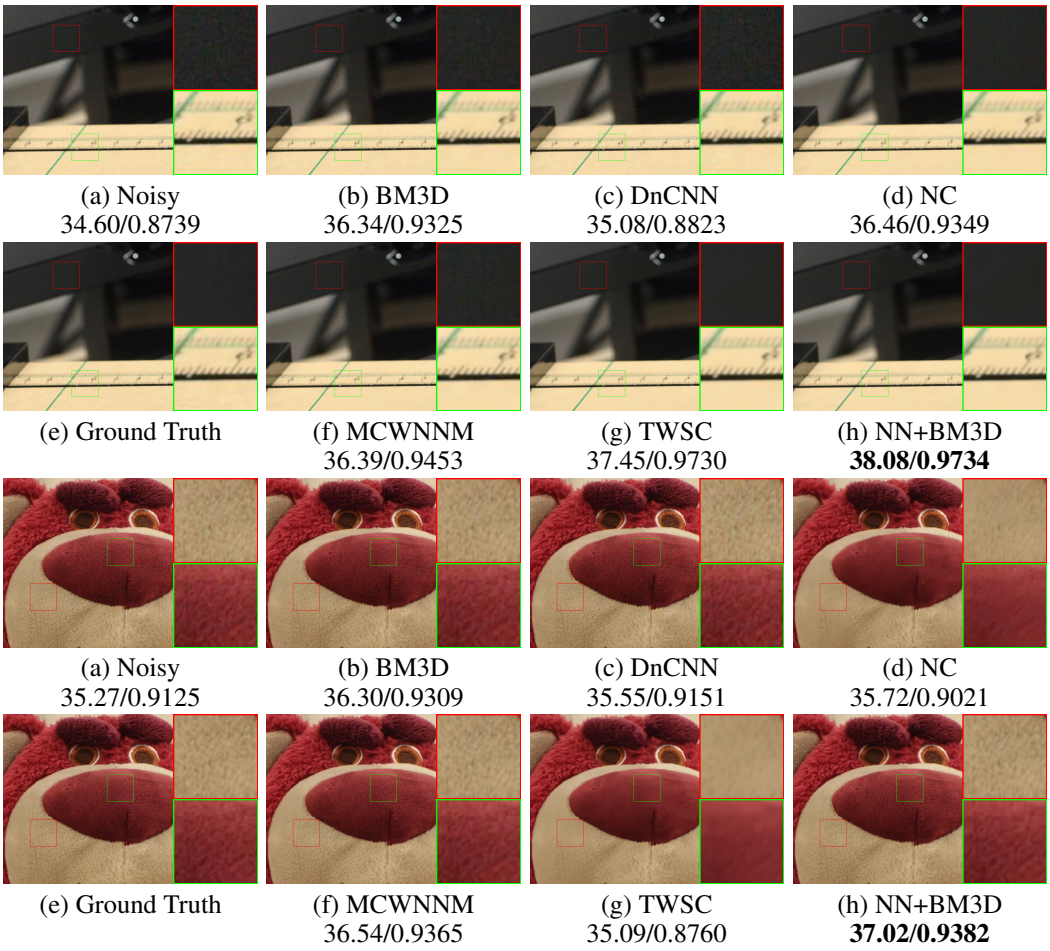

Figure 2: Visual results and PNSR/SSIM of five noisy images from PolyU.

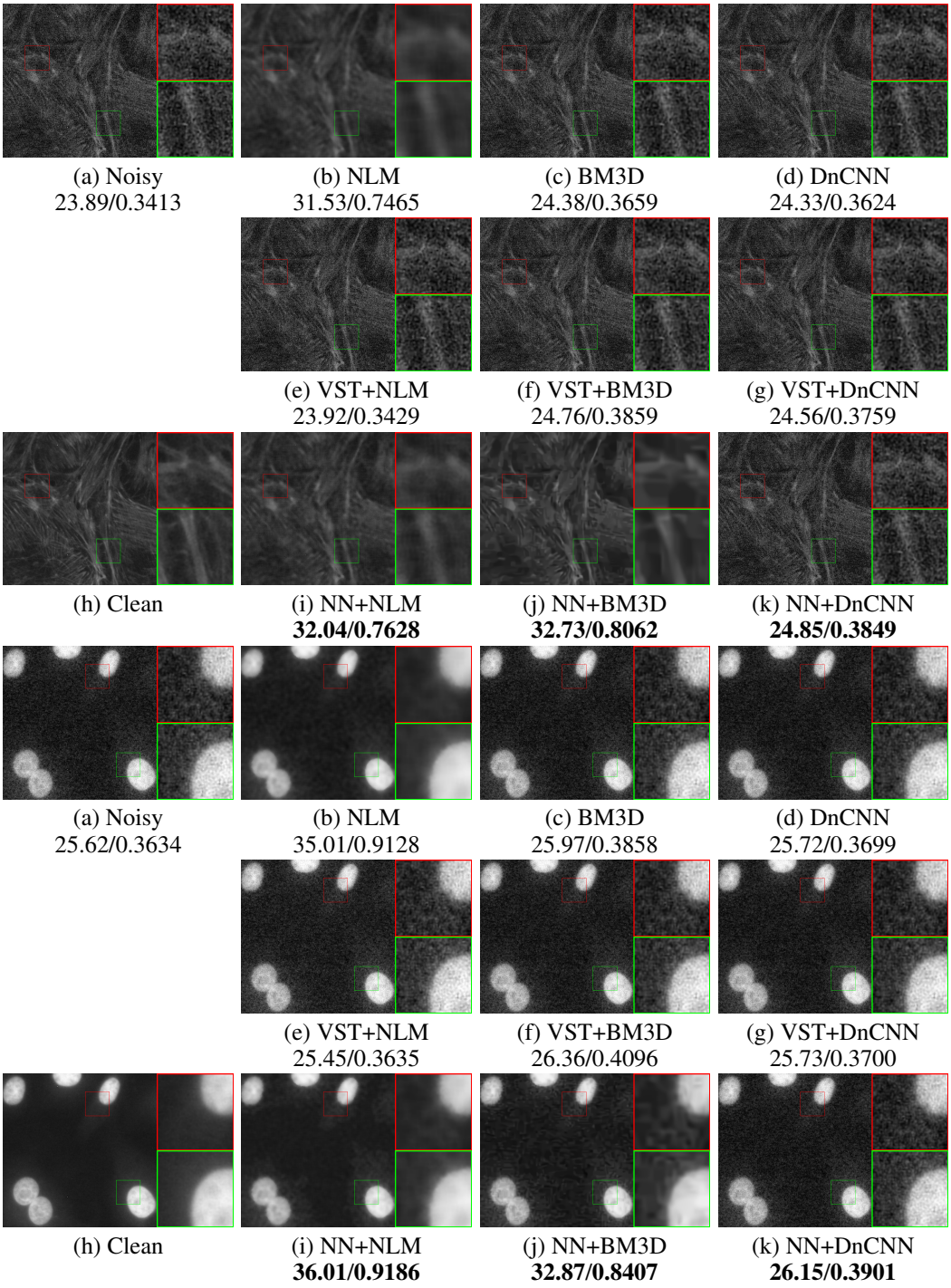

Figure 3: Visual results and PNSR/SSIM of two noisy images from FMDD.

(a) Noisy (b) BM3D (c) MCWNNM (d) NC

(e) VDN (f) DnCNN (g) FFDNet (h) NN+BM3D

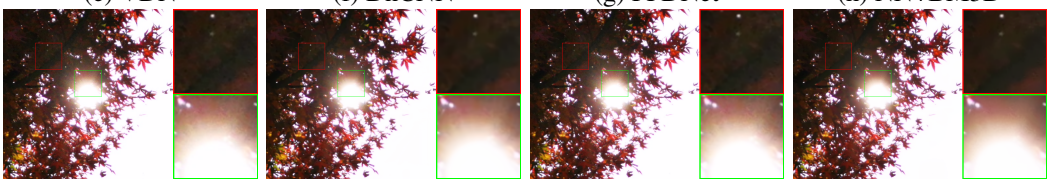

(a) Noisy (b) BM3D (c) MCWNNM (d) NC

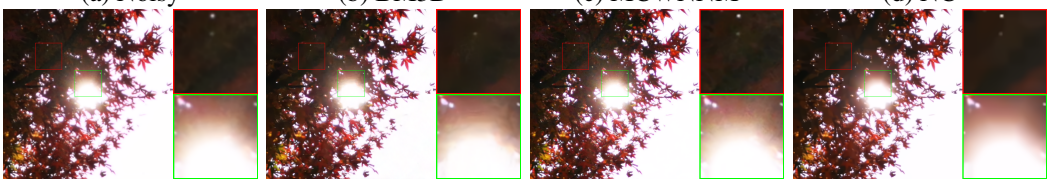

(e) VDN (f) DnCNN (g) FFDNet (h) NN+BM3D

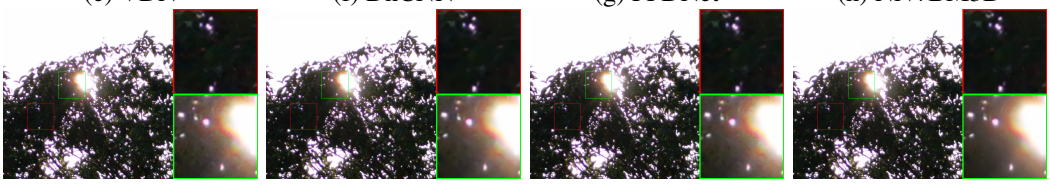

(a) Noisy (b) BM3D (c) MCWNNM (d) NC

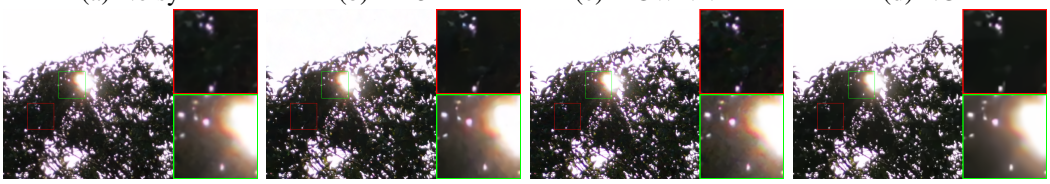

(e) VDN (f) DnCNN (g) FFDNet (h) NN+BM3D

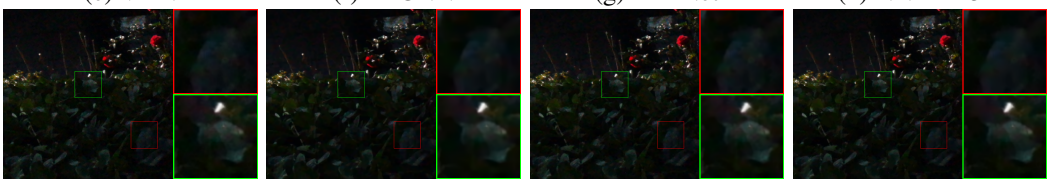

(a) Noisy (b) BM3D (c) MCWNNM (d) NC

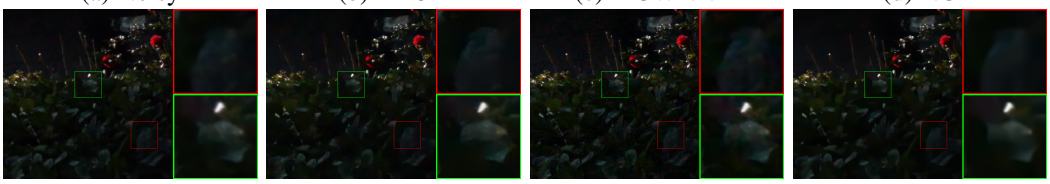

(e) VDN (f) DnCNN (g) FFDNet (h) NN+BM3D

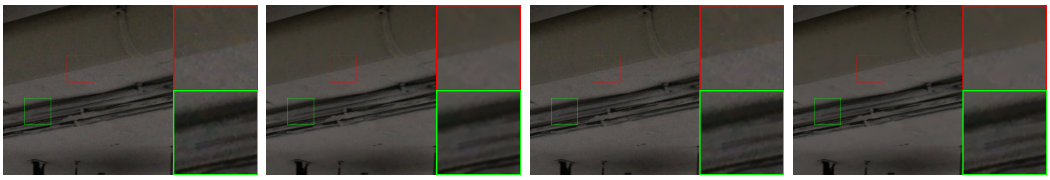

(a) Noisy (b) BM3D (c) MCWNNM (d) NC

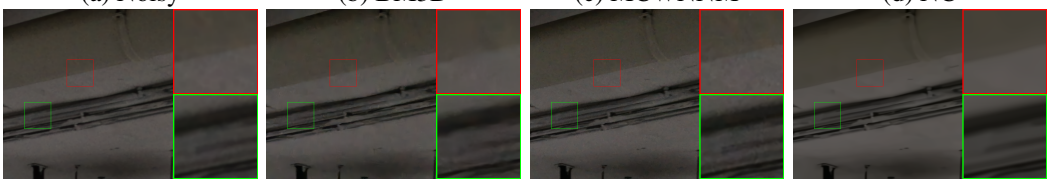

(e) VDN (f) DnCNN (g) FFDNet (h) NN+BM3D

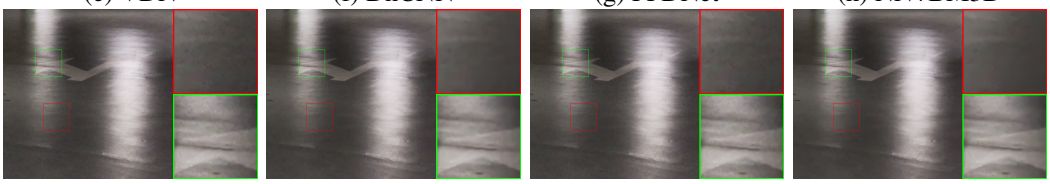

(a) Noisy (b) BM3D (c) MCWNNM (d) NC

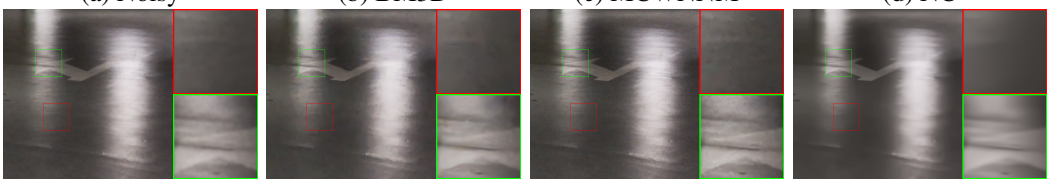

(e) VDN (f) DnCNN (g) FFDNet (h) NN+BM3D

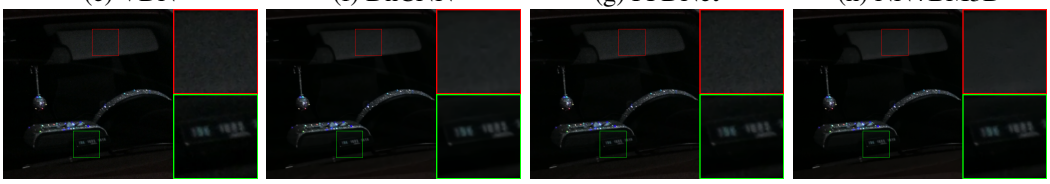

(a) Noisy (b) BM3D (c) MCWNNM (d) NC

(e) VDN (f) DnCNN (g) FFDNet (h) NN+BM3D

(a) Noisy (b) BM3D (c) MCWNNM (d) NC

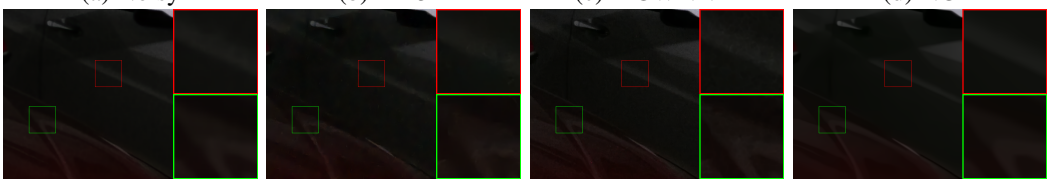

(e) VDN (f) DnCNN (g) FFDNet (h) NN+BM3D

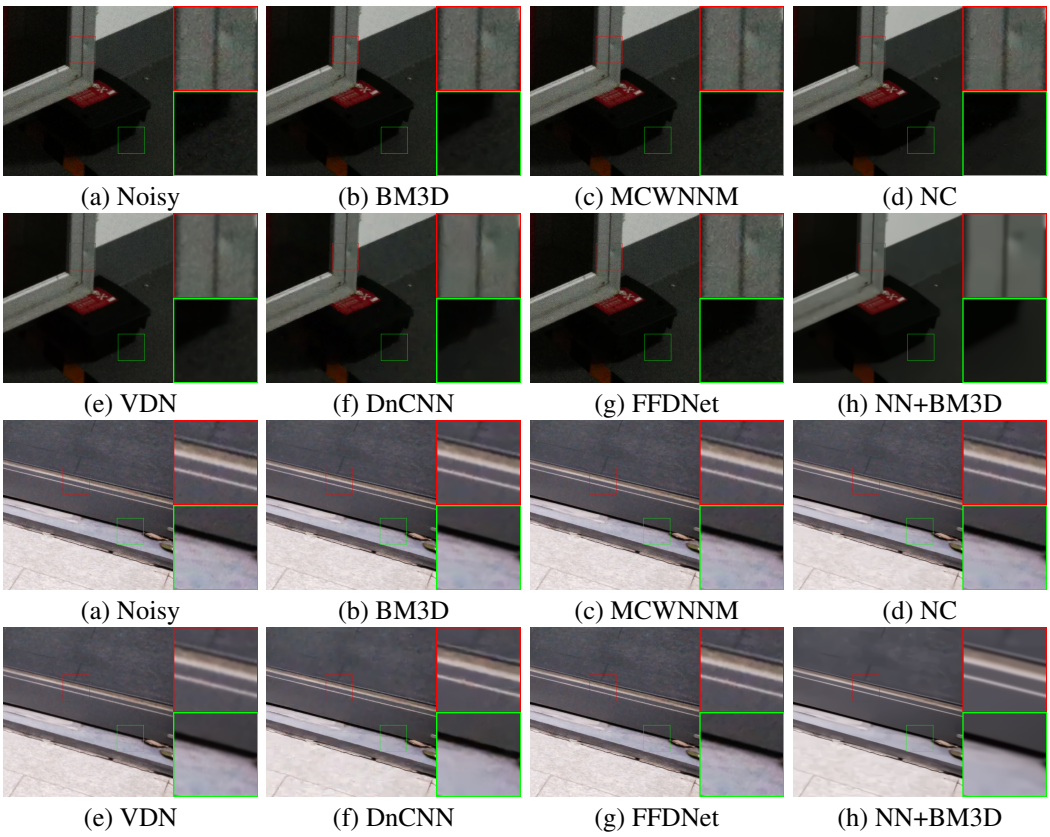

(a) Noisy (b) BM3D (c) MCWNNM (d) NC

(e) VDN (f) DnCNN (g) FFDNet (h) NN+BM3D

(a) Noisy (b) BM3D (c) MCWNNM (d) NC

(e) VDN (f) DnCNN (g) FFDNet (h) NN+BM3D

Figure 4: Visual results for real-world image denoising.

REFERENCES

Kostadin Dabov, Alessandro Foi, Vladimir Katkovnik, and Karen Egiazarian. Color image denoising via sparse 3d collaborative filtering with grouping constraint in luminance-chrominance space. In *ICIP*, volume 1, pp. I–313. IEEE, 2007.

Marc Lebrun, Miguel Colom, and Jean-Michel Morel. The noise clinic: a blind image denoising algorithm. *Image Processing On Line*, 5:1–54, 2015.

Markku Makitalo and Alessandro Foi. Optimal inversion of the generalized anscombe transformation for poisson-gaussian noise. *IEEE Trans. Image Process.*, 22(1):91–103, 2012.

Seonghyeon Nam, Youngbae Hwang, Yasuyuki Matsushita, and Seon Joo Kim. A holistic approach to cross-channel image noise modeling and its application to image denoising. In *CVPR*, pp. 1683–1691, 2016.

Jun Xu, Lei Zhang, David Zhang, and Xiangchu Feng. Multi-channel weighted nuclear norm minimization for real color image denoising. In *ICCV*, pp. 1096–1104, 2017.

Jun Xu, Hui Li, Zhetong Liang, David Zhang, and Lei Zhang. Real-world noisy image denoising: A new benchmark. *arXiv:1804.02603*, 2018a.

Jun Xu, Lei Zhang, and David Zhang. A trilateral weighted sparse coding scheme for real-world image denoising. In *ECCV*, pp. 20–36, 2018b.

Zongsheng Yue, Hongwei Yong, Qian Zhao, Deyu Meng, and Lei Zhang. Variational denoising network: Toward blind noise modeling and removal. In *NIPS*, pp. 1688–1699, 2019.

Kai Zhang, Wangmeng Zuo, Yunjin Chen, Deyu Meng, and Lei Zhang. Beyond a gaussian denoiser: Residual learning of deep cnn for image denoising. *IEEE Trans. Image Process.*, 26(7):3142–3155, 2017.

Kai Zhang, Wangmeng Zuo, and Lei Zhang. Ffdnet: Toward a fast and flexible solution for cnn-based image denoising. *IEEE Trans. Image Process.*, 27(9):4608–4622, 2018.

Yide Zhang, Yinhao Zhu, Evan Nichols, Qingfei Wang, Siyuan Zhang, Cody Smith, and Scott Howard. A poisson-gaussian denoising dataset with real fluorescence microscopy images. In *CVPR*, pp. 11710–11718, 2019.